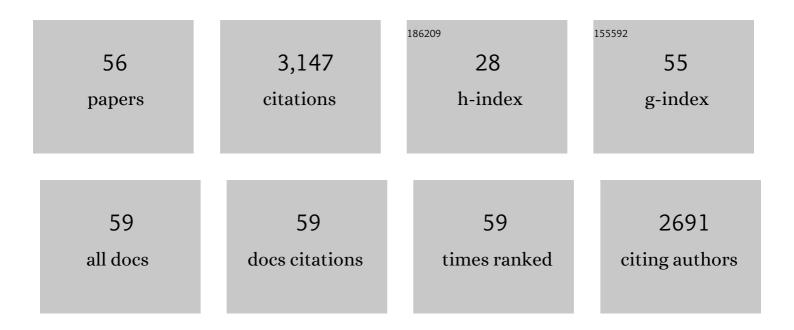
## **Alexey Silakov**

List of Publications by Year in descending order

Source: https://exaly.com/author-pdf/6838333/publications.pdf Version: 2024-02-01



#	Article	IF	CITATIONS
1	Using peptide substrate analogs to characterize a radical intermediate in NosN catalysis. Methods in Enzymology, 2022, 666, 469-487.	0.4	0
2	Use of Noncanonical Tyrosine Analogues to Probe Control of Radical Intermediates during Endoperoxide Installation by Verruculogen Synthase (FtmOx1). ACS Catalysis, 2022, 12, 6968-6979.	5.5	12
3	Mechanism of Reduction of an Aminyl Radical Intermediate in the Radical SAM GTP 3′,8-Cyclase MoaA. Journal of the American Chemical Society, 2021, 143, 13835-13844.	6.6	7
4	First Step in Catalysis of the Radical <i>S</i> -Adenosylmethionine Methylthiotransferase MiaB Yields an Intermediate with a [3Fe-4S] <sup>0</sup> -Like Auxiliary Cluster. Journal of the American Chemical Society, 2020, 142, 1911-1924.	6.6	21
5	Impact of Atomizer Age and Flavor on <i>In Vitro</i> Toxicity of Aerosols from a Third-Generation Electronic Cigarette against Human Oral Cells. Chemical Research in Toxicology, 2020, 33, 2527-2537.	1.7	12
6	Investigation of the Unusual Ability of the [FeFe] Hydrogenase from <i>Clostridium beijerinckii</i> to Access an O <sub>2</sub> -Protected State. Journal of the American Chemical Society, 2020, 142, 12409-12419.	6.6	29
7	Narrow-Spectrum Antibiotic Targeting of the Radical SAM Enzyme MqnE in Menaquinone Biosynthesis. Biochemistry, 2020, 59, 2562-2575.	1.2	10
8	An Unexpected Species Determined by X-ray Crystallography that May Represent an Intermediate in the Reaction Catalyzed by Quinolinate Synthase. Journal of the American Chemical Society, 2019, 141, 14142-14151.	6.6	6
9	Analysis of RNA Methylation by Phylogenetically Diverse Cfr Radical <i>S</i> -Adenosylmethionine Enzymes Reveals an Iron-Binding Accessory Domain in a Clostridial Enzyme. Biochemistry, 2019, 58, 3169-3184.	1.2	3
10	Ferredoxins as interchangeable redox components in support of MiaB, a radical Sâ€adenosylmethionine methylthiotransferase. Protein Science, 2019, 28, 267-282.	3.1	20
11	The Toxicity of Electronic Cigarette Vapor on Human Oral Cells. FASEB Journal, 2019, 33, 786.6.	0.2	ο
12	Two Distinct Mechanisms for C–C Desaturation by Iron(II)- and 2-(Oxo)glutarate-Dependent Oxygenases: Importance of α-Heteroatom Assistance. Journal of the American Chemical Society, 2018, 140, 7116-7126.	6.6	98
13	Structural Basis for Superoxide Activation of <i>Flavobacterium johnsoniae</i> Class I Ribonucleotide Reductase and for Radical Initiation by Its Dimanganese Cofactor. Biochemistry, 2018, 57, 2679-2693.	1.2	38
14	Effect of flavoring chemicals on free radical formation in electronic cigarette aerosols. Free Radical Biology and Medicine, 2018, 120, 72-79.	1.3	111
15	Metal-free class le ribonucleotide reductase from pathogens initiates catalysis with a tyrosine-derived dihydroxyphenylalanine radical. Proceedings of the National Academy of Sciences of the United States of America, 2018, 115, 10022-10027.	3.3	49
16	Evidence for a Di-μ-oxo Diamond Core in the Mn(IV)/Fe(IV) Activation Intermediate of Ribonucleotide Reductase from <i>Chlamydia trachomatis</i> . Journal of the American Chemical Society, 2017, 139, 1950-1957.	6.6	28
17	Characterization of a selenocysteine-ligated P450 compound I reveals direct link between electron donation and reactivity. Nature Chemistry, 2017, 9, 623-628.	6.6	62
18	Vanadyl as a Stable Structural Mimic of Reactive Ferryl Intermediates in Mononuclear Nonheme-Iron Enzymes. Inorganic Chemistry, 2017, 56, 13382-13389.	1.9	19

ALEXEY SILAKOV

#	Article	IF	CITATIONS
19	Visualizing the Reaction Cycle in an Iron(II)- and 2-(Oxo)-glutarate-Dependent Hydroxylase. Journal of the American Chemical Society, 2017, 139, 13830-13836.	6.6	97
20	Efficient methylation of C2 in l-tryptophan by the cobalamin-dependent radical S-adenosylmethionine methylase TsrM requires an unmodified N1 amine. Journal of Biological Chemistry, 2017, 292, 15456-15467.	1.6	33
21	Stable Open-Shell Phosphorane Based on a Redox-Active Amidodiphenoxide Scaffold. Inorganic Chemistry, 2017, 56, 8661-8668.	1.9	20
22	Characterization of Radical S-adenosylmethionine Enzymes and Intermediates in their Reactions by Continuous Wave and Pulse Electron Paramagnetic Resonance Spectroscopies. Biological Magnetic Resonance, 2017, , 143-186.	0.4	2
23	What Is the Preferred Conformation of Phosphatidylserine–Copper(II) Complexes? A Combined Theoretical and Experimental Investigation. Journal of Physical Chemistry B, 2016, 120, 12883-12889.	1.2	13
24	Structure of Quinolinate Synthase from <i>Pyrococcus horikoshii</i> in the Presence of Its Product, Quinolinic Acid. Journal of the American Chemical Society, 2016, 138, 7224-7227.	6.6	15
25	Unusual Synthetic Pathway for an {Fe(NO) <sub>2</sub> } <sup>9</sup> Dinitrosyl Iron Complex (DNIC) and Insight into DNIC Electronic Structure via Nuclear Resonance Vibrational Spectroscopy. Inorganic Chemistry, 2016, 55, 5485-5501.	1.9	55
26	Probing ligand-induced modulation of metallic states in small gold nanoparticles using conduction electron spin resonance. Physical Chemistry Chemical Physics, 2016, 18, 25443-25451.	1.3	19
27	Chain Length and Solvent Control over the Electronic Properties of Alkanethiolate-Protected Gold Nanoparticles at the Molecule-to-Metal Transition. Journal of the American Chemical Society, 2016, 138, 15987-15993.	6.6	27
28	Spectroscopic and Electrochemical Characterization of the Iron–Sulfur and Cobalamin Cofactors of TsrM, an Unusual Radical <i>S</i> -Adenosylmethionine Methylase. Journal of the American Chemical Society, 2016, 138, 3416-3426.	6.6	77
29	Direct Measurement of the Radical Translocation Distance in the Class I Ribonucleotide Reductase from <i>Chlamydia trachomatis</i> . Journal of Physical Chemistry B, 2015, 119, 13777-13784.	1.2	10
30	Ligand Control over the Electronic Properties within the Metallic Core of Gold Nanoparticles. Angewandte Chemie - International Edition, 2015, 54, 11750-11753.	7.2	26
31	Experimental Correlation of Substrate Position with Reaction Outcome in the Aliphatic Halogenase, SyrB2. Journal of the American Chemical Society, 2015, 137, 6912-6919.	6.6	78
32	Significantly shorter Fe–S bond in cytochrome P450-I is consistent with greater reactivity relative to chloroperoxidase. Nature Chemistry, 2015, 7, 696-702.	6.6	92
33	Structural, Electronic, and Magnetic Characterization of a Dinuclear Zinc Complex Containing TCNQ <sup>–</sup> and a μ-[TCNQ–TCNQ] <sup>2–</sup> Ligand. Inorganic Chemistry, 2015, 54, 6072	-6074.	6
34	Characterization of a Radical Intermediate in Lipoyl Cofactor Biosynthesis. Journal of the American Chemical Society, 2015, 137, 13216-13219.	6.6	17
35	Evaluating the Effectiveness of a Technological Compliance-Management System for the Production of Chemical Fibers. Fibre Chemistry, 2014, 46, 266-272.	0.0	1
36	Technology Compliance Management in Chemical Fibre Manufacture. Fibre Chemistry, 2014, 46, 136-142.	0.0	0

ALEXEY SILAKOV

#	Article	IF	CITATIONS
37	Characterization of a Cross-Linked Protein–Nucleic Acid Substrate Radical in the Reaction Catalyzed by RlmN. Journal of the American Chemical Society, 2014, 136, 8221-8228.	6.6	42
38	A 2.8 à Fe–Fe Separation in the Fe <sub>2</sub> <sup>III/IV</sup> Intermediate, X, from <i>Escherichia coli</i> Ribonucleotide Reductase. Journal of the American Chemical Society, 2013, 135, 16758-16761.	6.6	39
39	Iron(IV)hydroxide p <i>K</i> <sub>a</sub> and the Role of Thiolate Ligation in C–H Bond Activation by Cytochrome P450. Science, 2013, 342, 825-829.	6.0	283
40	A substrate radical intermediate in catalysis by the antibiotic resistance protein Cfr. Nature Chemical Biology, 2013, 9, 422-427.	3.9	45
41	Function of the Diiron Cluster of <i>Escherichia coli</i> Class Ia Ribonucleotide Reductase in Proton-Coupled Electron Transfer. Journal of the American Chemical Society, 2013, 135, 8585-8593.	6.6	55
42	Importance of the Protein Framework for Catalytic Activity of [FeFe]-Hydrogenases. Journal of Biological Chemistry, 2012, 287, 1489-1499.	1.6	129
43	Identification and Characterization of the "Superâ€Reduced―State of the Hâ€Cluster in [FeFe] Hydrogenase: A New Building Block for the Catalytic Cycle?. Angewandte Chemie - International Edition, 2012, 51, 11458-11462.	7.2	184
44	EPR/ENDOR, Mössbauer, and Quantum-Chemical Investigations of Diiron Complexes Mimicking the Active Oxidized State of [FeFe]Hydrogenase. Inorganic Chemistry, 2012, 51, 8617-8628.	1.9	28
45	Magnetic Properties of [FeFe]â€Hydrogenases: A Theoretical Investigation Based on Extended QM and QM/MM Models of the H luster and Its Surroundings. European Journal of Inorganic Chemistry, 2011, 2011, 1043-1049.	1.0	21
46	Unraveling the Electronic Properties of the Photoinduced States of the H-Cluster in the [FeFe] Hydrogenase from D. desulfuricans. European Journal of Inorganic Chemistry, 2011, 2011, 1056-1066.	1.0	23
47	A Model of the [FeFe] Hydrogenase Active Site with a Biologically Relevant Azadithiolate Bridge: A Spectroscopic and Theoretical Investigation. Angewandte Chemie - International Edition, 2011, 50, 1439-1443.	7.2	130
48	The [FeFe]â€hydrogenase maturase HydF from <i>Clostridium acetobutylicum</i> contains a CO and CN <sup>â^'</sup> ligated iron cofactor. FEBS Letters, 2010, 584, 638-642.	1.3	94
49	Advanced Electron Paramagnetic Resonance and Density Functional Theory Study of a {2Fe3S} Cluster Mimicking the Active Site of [FeFe] Hydrogenase. Journal of the American Chemical Society, 2010, 132, 17578-17587.	6.6	19
50	Spin distribution of the H-cluster in the Hox–CO state of the [FeFe]Âhydrogenase from Desulfovibrio desulfuricans: HYSCORE and ENDOR study of 14N and 13C nuclear interactions. Journal of Biological Inorganic Chemistry, 2009, 14, 301-313.	1.1	43
51	Spectroelectrochemical Characterization of the Active Site of the [FeFe] Hydrogenase HydA1 from <i>Chlamydomonas reinhardtii</i> . Biochemistry, 2009, 48, 7780-7786.	1.2	133
52	14N HYSCORE investigation of the H-cluster of [FeFe] hydrogenase: evidence for a nitrogen in the dithiol bridge. Physical Chemistry Chemical Physics, 2009, 11, 6592.	1.3	354
53	Optimized over-expression of [FeFe] hydrogenases with high specific activity in Clostridium acetobutylicum. International Journal of Hydrogen Energy, 2008, 33, 6076-6081.	3.8	77
54	Isolation and first EPR characterization of the [FeFe]-hydrogenases from green algae. Biochimica Et Biophysica Acta - Bioenergetics, 2008, 1777, 410-416.	0.5	104

#	Article	IF	CITATIONS
55	The Electronic Structure of the H-Cluster in the [FeFe]-Hydrogenase from <i>Desulfovibrio desulfuricans</i> : A Q-band <sup>57</sup> Fe-ENDOR and HYSCORE Study. Journal of the American Chemical Society, 2007, 129, 11447-11458.	6.6	157
56	A pulsed EPR study of clustering of Yb3+ ions incorporated in GeO2 glass. Journal of Non-Crystalline Solids, 2004, 333, 22-27.	1.5	30